Toxicology and Applied Pharmacology 232 (2008) 292–301

Contents lists available at ScienceDirect

Toxicology and Applied Pharmacology

journal homepage: www.elsevier.com/locate/ytaap

Integrated metabolomic analysis of the nano-sized copper particle-induced hepatotoxicity and nephrotoxicity in rats: A rapid *in vivo* screening method for nanotoxicity

Ronghui Lei [a,b], Chunqi Wu [a], Baohua Yang [a], Huazhai Ma [a], Chang Shi [a], Quanjun Wang [a], Qingxiu Wang [a], Ye Yuan [a], Mingyang Liao [a,*]

[a] National Beijing Center for Drug Safety Evaluation and Research, Beijing Institute of Pharmacology and Toxicology, 27 Taiping Road, Beijing 100850, PR China
[b] Department of Public Health, Xi'an Jiaotong University, Xi'an 710061, PR China

ARTICLE INFO

Article history:
Received 15 March 2008
Revised 27 June 2008
Accepted 28 June 2008
Available online 26 July 2008

Keywords:
Nano-copper
Hepatotoxicity and nephrotoxicity
Metabolomics
Nuclear magnetic resonance (NMR)
Principal component analysis (PCA)

ABSTRACT

Despite an increasing application of copper nanoparticles, there is a serious lack of information concerning their impact on human health and the environment. In this study, the biochemical compositions of urine, serum, and extracts of liver and kidney tissues of rats treated with nano-copper at the different doses (50, 100, and 200 mg/kg/d for 5 d) were investigated using ^{1}H NMR techniques with the pattern recognition methods. Serum biochemical analysis and histopathological examinations of the liver and kidney of all the rats were simultaneously performed. All the results indicated that the effects produced by nano-copper at a dose of 100 or 50 mg/kg/d were less than those induced at a higher dose of 200 mg/kg/d. Nano-copper induced overt hepatotoxicity and nephrotoxicity at 200 mg/kg/d for 5 d, which mainly involved scattered dot hepatocytic necrosis and widespread renal proximal tubule necrosis. Increased citrate, succinate, trimethylamine-*N*-oxide, glucose, and amino acids, accompanied by decreased creatinine levels were observed in the urine; furthermore, elevated levels of lactate, 3-hydroxybutyrate, acetate, creatine, triglycerides, and phosphatide and reduced glucose levels were observed in the serum. The predominant changes identified in the liver tissue aqueous extracts included increased lactate and creatine levels together with reduced glutamine and taurine levels, and the metabolic profile of the kidney tissue aqueous extracts showed an increase in lactate and a drop in glucose. In the chloroform/methanol extracts of the liver and kidney tissues, elevated triglyceride species were identified. These changes suggested that mitochondrial failure, enhanced ketogenesis, fatty acid β-oxidation, and glycolysis contributed to the hepatotoxicity and nephrotoxicity induced by nano-copper at 200 mg/kg/d for 5 d. An increase in triglycerides in the serum, liver and kidney tissues could serve as a potential sensitive biomarker reflecting the lipidosis induced by nano-copper. The data generated from the current study completely supports the fact that an integrated metabolomic approach is promising for the development of a rapid *in vivo* screening method for nanotoxicity.

Introduction

The rapid growth of nanotechnology suggests that it will soon find wide application in daily consumer products and new pharmaceutical, electronic, and other industries. However, to date, there is still a lack of information regarding the human health and environmental implications of manufactured nanomaterials (Colvin, 2003). For successful application of nanomaterials in bioscience, it is important to understand the biological fate and potential toxicity of nanoparticles. Copper is an essential trace element capable of producing toxic effects in animals or humans when ingested acutely or chronically, in excess (Bremner, 1998). There are numerous data regarding the toxicity of copper compounds. After oral exposure, the gastrointestinal system, liver, and kidneys are sensitive targets of copper toxicity. The manifestation of Cu poisoning mainly includes drowsiness and anorexia in the early stages (Semple et al., 1960; Winge and Mehra, 1990) as well as disruption of the epithelial lining of the gastrointestinal tract, hepatocellular necrosis, and acute tubular necrosis in the kidney (Barceloux, 1999). Copper nanoparticles (nano-copper) have shown great promise as osteoporosis-treatment drugs, antibacterial materials, additives in livestock and poultry feed, and intrauterine contraceptive devices. Furthermore, nano-copper has been widely used in industry, e.g., as an additive in lubricants (Liu et al., 2004), for metallic coating (Cioffi et al., 2005), and as a highly reactive catalyst in organic hydrogen reactions. Usually, a variation in the size of metal nanoparticles results in bare nanoparticles possessing excessive surface

* Corresponding author. Fax: +86 10 68159974.
E-mail address: liaomingy@hotmail.com (M. Liao).

0041-008X/$ – see front matter © 2008 Elsevier Inc. All rights reserved.
doi:10.1016/j.taap.2008.06.026

energy, and this leads to an alteration in their catalytic properties (Bakunin et al., 2004). This means that the dissolution of metal nanoparticles would occur once conditions are appropriate. Hence, for toxicology research in metal nanoparticles, it is essential to distinguish between the effects of nanoparticulates from dissolved metals. A recent report demonstrated that when mice were acutely exposed to nano-copper or micro-copper particles, only nano-copper particles induced severe impairment in the kidney, liver, and spleen in mice (Chen et al., 2006). Further study revealed that the toxicity of nano-sized copper particles was highly correlated with the particle size/specific surface area. Compared to micro-copper (17 μm), nano-copper (23.5 nm) can rapidly interact with artificial gastric acid juice and be transformed into ionic copper with ultrahigh reactivity. Moreover, metabolic alkalosis and copper accumulation in the kidneys was detected in mice that were orally exposed to nano-copper particles (Meng et al., 2007).

Although the potential risks of nano-copper particles on human health have been identified, subacute toxicity of it has not been described. Currently, systemic biological approaches (genomics, proteomics, and metabonomics/metabolomics) have been widely applied in the toxicology research field and have provided valuable information in this regard. Among of them, metabolomics is a rapidly developing new discipline which is the collection of the global metabolic data and their interpretation (both spectral and biochemical) using modern spectroscopic techniques and appropriate statistical approaches. It may provide us with better, more useful information with higher throughput at a lower cost than genomics, transcriptomics or proteomics. Thus far, a variety of spectroscopic techniques have been used to generate metabolomic data sets, such as nuclear magnetic resonance (NMR) spectroscopy, liquid chromatography coupled mass spectrometry (LC–MS), tandem and Fourier-transform mass spectrometry, capillary electrophoresis and infrared spectroscopy (Nicholson et al., 2002; Serkova and Niemann, 2006; Dunn et al., 2005; Want et al., 2007). In contrast with other means, ^{1}H-NMR has two significant advantages. One is its nonselectivity in metabolite detection and ability of multiple metabolite quantification, the other is the minimal sample preparation required. It enables detection of all soluble proton-containing small-molecular-weight metabolites less than 1000 Da that are present in concentrations above 10 μM, providing both quantitative and structural information. Given the amount and complexity of spectroscopic data from NMR studies, pattern recognition approaches and chemometric analysis were usually used to implement the interpretation of spectral data (Anthony et al., 1992; Gartland et al., 1991; Holmes et al., 1998, 2000). Principal component analysis (PCA) is one such routinely used pattern recognition method where the NMR spectra are reduced to a set of peak intensity descriptors and analyzed to identify similarities and differences in biochemical characteristics between control and treated animals. Compared to the traditional techniques, the prominent advantages of NMR-based metabolomic approach include timesaving, sensitive, non- or less invasive and holistic view of the biochemical variations. So, it has been widely used in the toxicity evaluations of candidate drugs (Waterfield et al., 1993; Robertson et al., 2000; Nicholson et al., 2002). Recent studies also showed that integrated metabolomic approach is useful in mechanistic toxicological studies (Waters et al., 2006; Yap et al., 2006).

In this study, the biochemical effects of nano-copper were investigated by examining urine, serum, and liver and kidney tissue extracts obtained from the rats repeatedly exposed to different doses of nano-copper by the ^{1}H NMR-PCA-based integrated metabolomic approach. Conventional clinical chemistry and histopathological examination were also performed at the same time in order to identify the toxic threshold, reveal the characteristics of the hepato- and nephrotoxicity induced by the nano-copper, identify potential toxic biomarkers, and evaluate the suitability of metabolomic approach as a rapid *in vivo* screening method for nanotoxicity.

Materials and methods

Characterization of copper particles. The 25-nm primary copper particles were commercially available from Shenzhen Zunye NanoMaterial Co. Ltd (Shenzhen, China). The preparation of suspensions of nano-copper particles was conducted by referring to previous literature (Chen et al., 2006). Prior to animal experiments, the size distribution of 25 nm copper particles in a 1% (w/v) hydroxypropylmethyl cellulose (HPMC) solution (K4M, Shanghai Colorcon Coating Technology Ltd., China) was analyzed using a dynamic light scattering particle size analyzer (LB-550 HORIBA, Japan) and atom force microscopy (Daojin Co., Japan). The dissolution of 25-nm Cu in the administrated solution was performed by inductively coupled plasma-atomic absorption spectrometry (ICP-AAS-7000, Daojin Co., Japan). The specific surface area was determined with a BET surface area analyzer (ASAT 2020 M+C Micromeritics, USA). The impurities (e.g. Al, Ba, Ca, Cd, Cr, Fe, Mg, Mn, Mo, Na, Ka, Ni, Pb, Sr, Zn, etc.) were analyzed by X-ray fluorescence spectroscopy (XRFS).

Dissolution of copper nanoparticles in artificial gastric fluid in vitro. In order to evaluate the dissolution of nano-copper in gastric fluid, 40 mg nano-copper was suspended in 2 ml 1% (w/v) HPMC solution, 30 ml artificial gastric fluid was then added (0.2% sodium chloride, 0.32% pepsin, 0.07% hydrochloric acid, pH 2) at 37 °C, and the suspension stirred for 5, 10, 15, 30, 45, 60, and 120 min. The 5 ml supernatant was collected and the copper content was analyzed by inductively coupled plasma-atomic absorption spectrometry (ICP-AAS-7000, Daojin Co. Japan). The mean of 3 determinations was used calculate the dissolution percentage of nano-copper in the artificial gastric fluid.

Animals. All animal experimental protocols complied with the local animal care guidelines. Male Wistar rats (200±10 g, Beijing, Weitonglihua, China) were housed in individual metabolic cages with free access to food and drinking water ad libitum. Environment conditions were set at 25±3 °C with a relative humidity of 50±10%, and a cycle of 12 h each light/dark. After 1 week acclimatization, weight-matched rats were randomly assigned to 4 groups.

Clinical chemistry. Clinical chemistry analysis of serum samples was carried out with a Hitachi 7020 Automatic Analyzer using appropriate kits. The following parameters were tested: alanine aminotransferase (ALT), aspartate aminotransferase (AST), alkaline phosphatase (ALP), total protein (TP), albumin (ALB), glucose (GLU), total cholesterol (TCHOL), triglyceride (TG), total bilirubin (TBILI), total bile acid (TBA), blood urea nitrogen (BUN), and creatinine (Crn).

Histopathology. Liver and kidney samples were fixed in 10% formalin and further processed for light microscopy. All sections were stained with hematoxylin and eosin and evaluated in a nonblinded fashion.

Metabolomic study of the hepatotoxicity and nephrotoxicity of nano-sized copper. Male Wistar rats were administered nano-copper suspensions daily at doses of 50, 100, and 200 mg/kg body weight or vehicle (1% HPMC) by oral gavage for 5 d (10 mL/kg, n=6 per group), respectively. For the purpose of this experiment, a study day refers to each 24 h period following dosing. Urine samples were collected in ice-cooled vessels containing 1% sodium azide (0.1 ml) at 24 h pretest and then days 1 and 5 and immediately frozen at −80 °C prior to NMR analysis. All rats were euthanized under diethyl ether anesthesia on Day 6. Blood (3–4 mL) was collected from the femoral artery and serum was separated by centrifugation at 2000×g for 15 min at 4 °C. Serum samples (0.5 mL) were immediately used for clinical biochemical analysis, and the remaining were duplicated and frozen at −80 °C for the following NMR spectroscopy. The tissue

collection was reference to the literature (Atherton et al., 2006; Maxwell et al., 1998). In brief, the liver and kidney were immediately removed from each animal postmortem and weighed. Then excised samples that weighed approximately 250 mg from the left lateral liver lobe and the right kidney, respectively, were immediately snap-frozen in liquid nitrogen for NMR analysis. The remaining left lateral liver lobe and the left kidney were used for histopathological examination. The procedures of both tissue-weighing and -excising are carried out on ice-bath, and the time was controlled within 60 s postmortem time before freezing, snap-frozen in liquid nitrogen.

^{1}H NMR spectroscopy of urine. The preparation of the urine for NMR analysis was based on previous literature (Robertson et al., 2000). Aliquots (400 μl) of rat urine was added to 200 μl buffer solution (0.2 M sodium phosphate, pH 7.4); the urine-buffer mixture was left to stand for 10 min and then centrifuged at 3000×*g* at 4 °C for a further 10 min to remove any precipitate. The supernatant (500 μl) was then pipetted into a 5 mm NMR tube together with 50 μl of a 1 mg/ml solution of 3-trimethylsilylpropionic-(2,2,3,3-d4)-acid (TSP) in D_2O. The D_2O and TSP provided the deuterium lock signal for the NMR spectrometer and the chemical shift reference (δ 0.0), respectively. The urine samples were analyzed by ^{1}H NMR spectroscopy at 600.03 MHz using a Varian INOVA-600 spectrometer. One dimensional spectrum was acquired using a standard NOESY pulse sequence with water suppression during a relaxation delay of 2 s and mixing time of 150 ms. Sixty-four free induction decays (FID) were represented by 64 K data points with a spectral width of 7002.8 Hz, an acquisition time of 4.68 s, and a total pulse recycle delay of 6.68 s. The FIDs were multiplied by an exponential weighting function corresponding to a line broadening of 0.5 Hz prior to Fourier transformation (FT).

^{1}H NMR spectroscopy of serum. The preparation and NMR analysis of the serum samples were conducted as previously reported in the literature (Waters et al., 2005; Lindon et al., 2005). Serum (400 μl) was mixed with 200 μl D_2O and 100 μl of a 1 mg/ml solution of TSP in D_2O and then transferred into 5 mm NMR tubes. Samples were analyzed by ^{1}H NMR spectroscopy at 600.03 MHz using a Varian INOVA-600 spectrometer. Two types of ^{1}H NMR spectra were acquired for each sample. Water-suppressed Carr–Purcell–Meiboom–Gill (CPMG) spectra were acquired using the pulse sequence. This acts as a T_2 relaxation filter to suppress signals from macromolecular motion and other molecules with constrained molecular motions. Water-suppressed diffusion-edited were acquired to remove peaks from low-molecular weight components by using the bipolar-pair longitudinal–decay–current (BPP–LED) pulse sequence.

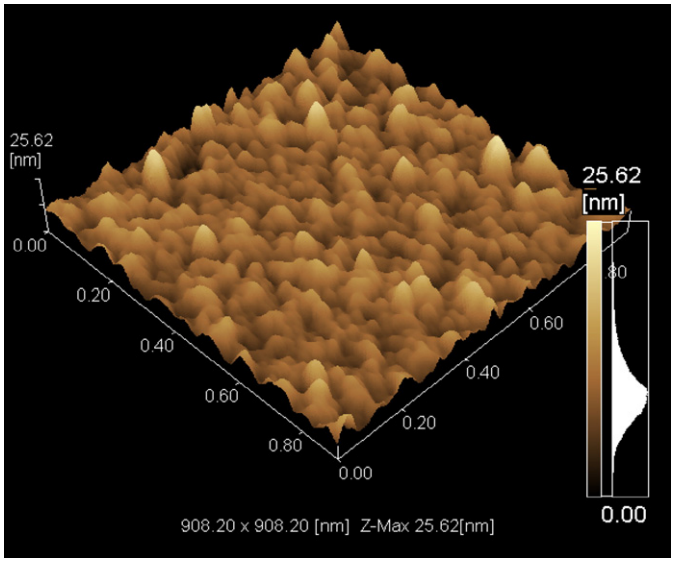

Fig. 1. AFM graph of 25-nm Cu particles in 1% hydroxypropylmethyl cellulose solution.

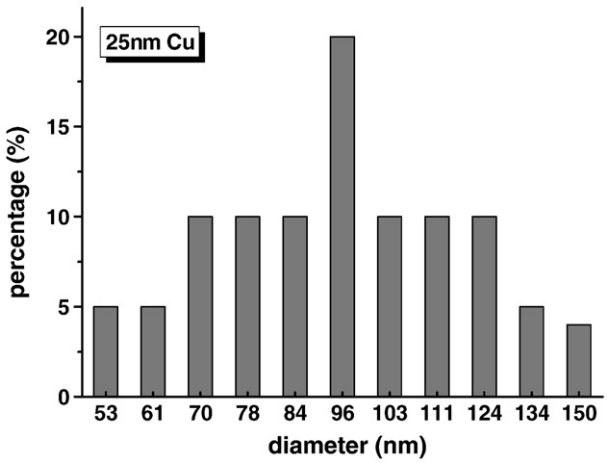

Fig. 2. Size distribution of 25-nm Cu particles in 1% hydroxypropylmethyl cellulose solution.

^{1}H NMR spectroscopy of liver and kidney tissue (Coen et al., 2004). Preweighed liver and kidney samples (250 mg) were homogenized in 2 ml of 50% acetonitrile and then centrifuged at 5070×*g* for 6 min at 4 °C. The supernatant was collected, lyophilized, and reconstituted in 0.5 ml D_2O prior to NMR analysis. Two milliliters of 75% CH_3CL_3/25% CH_3OH was added to the pellets, and the extraction was followed by a further centrifugation (5070×*g* for 15 min at 4 °C). The lipophilic supernatants were removed, dried under a stream of nitrogen, and reconstituted in 500 μl of 100% CH_3CL_3 prior to NMR analysis. The reconstituted solutions were transferred to 5 mm NMR tubes together with 30 μl of 10% TSP solution in D_2O. ^{1}H NMR spectra were acquired from each sample at 600.03 MHz on a Varian INOVA-600 spectrometer at 298 K. 1D NOESY pulse sequence was used to achieve satisfactory water suppression in the aqueous extracts. For each sample, 128 transients were collected into 64 K data points with a relaxation delay of 2 s and a mixing period of 150 ms. A spectral width of 9612 Hz and an acquisition time per scan of 3.32 s were used.

Data reduction and principal component analysis. All spectra were manually rephased, baseline corrected, and then data-reduced to 225 segments, each with a 0.04 ppm width for a spectral window ranging from 0.5 to 9.5 ppm using the VNMR 6.1C software package (Varian, Inc.). The segments of δ 6.2–4.6 ppm in the urine spectra were removed to exclude the uncertainty of the residual water signal and urea. The segments of δ 5.1–4.7 ppm in serum CPMG spectra and tissue aqueous extract spectra were removed to eliminate the artifacts of the residual water resonance. In case of the chloroform/methanol tissue extract, the spectra were divided into 150 segments, each 0.04 ppm wide for a spectral window ranging from 0.5 to 6.5 ppm, the segments 3.32–3.44 and 3.94–4.6 ppm were excluded to remove variation in water suppression efficiency. All remaining spectral segments were scaled to the total integrated area of the spectrum to reduce variation in concentration (Holmes et al., 1994).

The 1D ^{1}H NMR spectral data sets were imported into the SIMCA-P10.0 software package (Version 10, Umetrics AB, Umea, Sweden) separately. The data were then mean-centered and pareto-scaled prior to PCA. Two-dimensional score plots were used to visualize the separation of the samples and the corresponding loading plots were used to identify the spectral variable contribution to the position of the samples in the score plot.

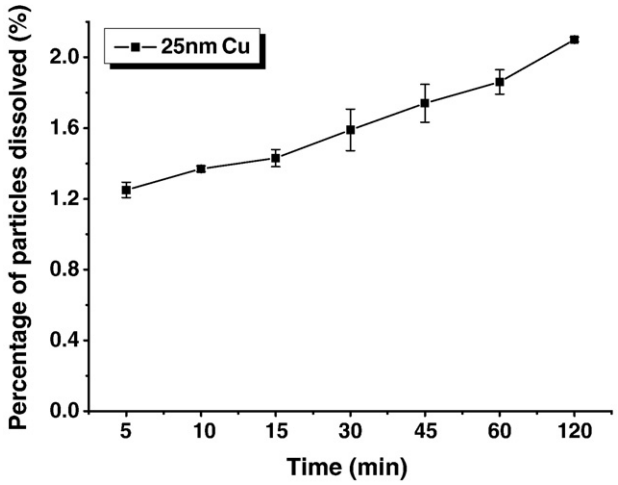

Fig. 3. Dissolution rate of 25-nm Cu particles in the artificial gastric fluid.

Statistics. The data from serum clinical chemistry analysis were expressed as the mean±SD. Statistical comparisons were performed using analysis of variance (ANOVA) followed by Newman–Keul's multiple comparison test. The criterion for statistical significance was set at $P<0.05$ or $P<0.01$.

Results

Nano-sized copper particle properties

The mean size of 25-nm primary copper particles was measured as 5~60 nm. Both the AFM graph (Fig. 1) and the result of dynamic light scattering analysis (Fig. 2) indicated that nano-copper particles could not be dispersed individually by 30-min ultrasonication in 1% HPMC solution, and their mean aggregation size was approximately 90 nm. The N_2-BET specific surface area was 6.92 m^2/g. The purity of nano-copper was no less than 99.9%. The dissolution rate of the nano-copper particles was 0.014±0.002% in 1% HPMC suspension solutions following 30-min ultrasonication. In addition, the 25-nm copper exhibited a rapid dissolution in the artificial gastric fluid. The percentage of particles dissolved immediately was 1.2% at the first detection time point of 5 min. Thereafter, the dissolution rate showed a slow, gradual rise to 2.1% at 2 h (Fig. 3).

General toxicity

Symptoms of gastrointestinal dysfunction, such as anorexia and severe diarrhea, were observed in all rats that were administered a 200 mg/kg nano-copper dose. Drowsiness, hypopnea, tremors, and arching of back were observed in 4 of 6 rats. No abnormalities were observed in the other treated groups and the control group during the study period.

The rats that were administered 200 mg/kg nano-copper for 5 d showed a dramatic weight loss. The average weight of the kidneys significantly increased in this group in comparison to the control group (Table 1).

Table 1
Effects of nano-sized copper on body-weight gain and organ weights (mean±SD)

Group	Control	Nano-copper (mg/kg)		
		50	100	200
Bodyweight gain(g)	5.50±5.79	11.33±14.02	0.83±11.67	−54.33±15.24**
Liver (g)	7.19±0.39	8.28±1.64	6.81±1.19	7.13±0.95
Kidney (g)	1.88±0.22	2.01±0.17	1.89±0.13	2.21±0.49*

Statistics: (*) $p<0.05$, (**) $p<0.01$ ($n=6$ for all groups).

Table 2
Effects of nano-sized copper on serum clinical chemistry parameters (mean±SD)

Parameters	Control	Nano-copper(mg/kg)		
		50	100	200
ALT (U/l)	34.83±2.64	30.17±5.00	27.50±6.28	131.67±104.94**
AST (U/l)	117.17±24.90	108.17±21.87	103.67±6.19	1345.33±854.96**
ALP (U/l)	138.17±16.45	132.50±31.84	133.50±23.30	105.17±77.71*
TP(g/l)	52.50±2.35	51.38±1.64	51.45±1.41	70.30±20.81*
ALB(g/l)	33.00±0.91	32.07±0.52	31.78±0.71	32.60±3.41
TCHOL(μM)	1.43±0.22	1.90±0.36*	1.97±0.24*	1.09±0.17*
TG(mM)	0.29±0.07	0.54±0.13*	0.54±0.06*	0.96±0.33**
GLU(mM)	6.48±1.39	5.08±0.47	4.86±0.40	4.81±1.93
TBA(μM)	7.83±0.60	8.40±1.75	8.93±2.53	17.88±8.80**
TBILI (μM)	3.25±0.73	3.93±3.81	4.03±1.54	88.77±65.40**
BUN (mM)	5.23±0.84	5.02±0.83	6.66±1.98	28.09±10.54**
Crn(μM)	22.63±3.65	19.65±3.94	23.50±4.39	270.63±97.77**

Statistics: (*) $p<0.05$, (**) $p<0.01$ ($n=6$ for all groups).

Clinical chemistry and histopathological examination

Significant changes in the serum clinical biochemistry parameters were restricted to the group treated with a high dose of nano-copper (Table 2). Aspartate aminotransferase, total bilirubin, blood urea nitrogen, and creatinine in the 200 mg/kg group increased significantly (over 5-fold) compared to the control group, and alanine aminotransferase, triglyceride and total bile acid increased to a lesser extent (beyond 2-fold). Additionally, alkaline phosphatase and total cholesterol were slightly reduced while total cholesterol and triglyceride were found to be elevated slightly in the mid- and low-dose groups.

Comparison of hematoxylin and eosin liver sections obtained from the control and nano-copper-treated rats indicated scattered dot

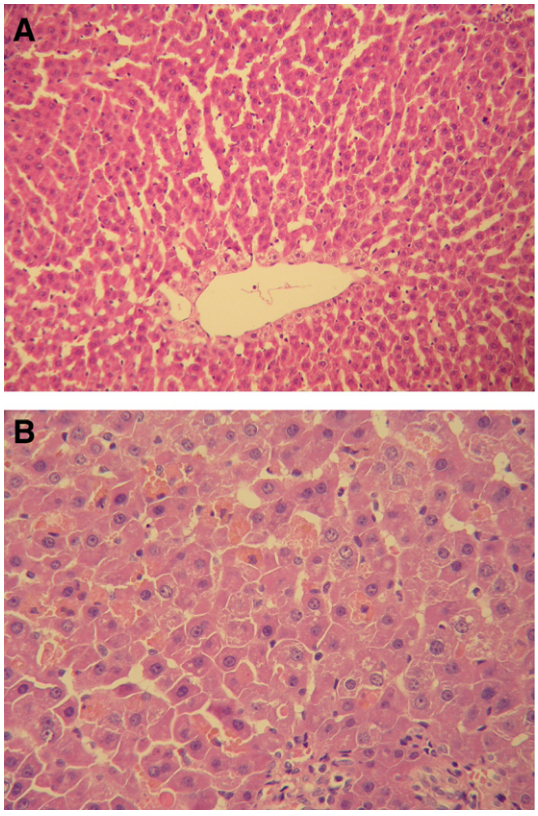

Fig. 4. Photomicrographs of rat livers of rats on day 6 after administration (HE stain). (A) Control rats exhibited normal morphology. Magnification, 200×. (B) The high-dose nano-copper-treated (200 mg/kg/d) rat exhibited scattered dot hepatocytic necrosis. Magnification, 400×.

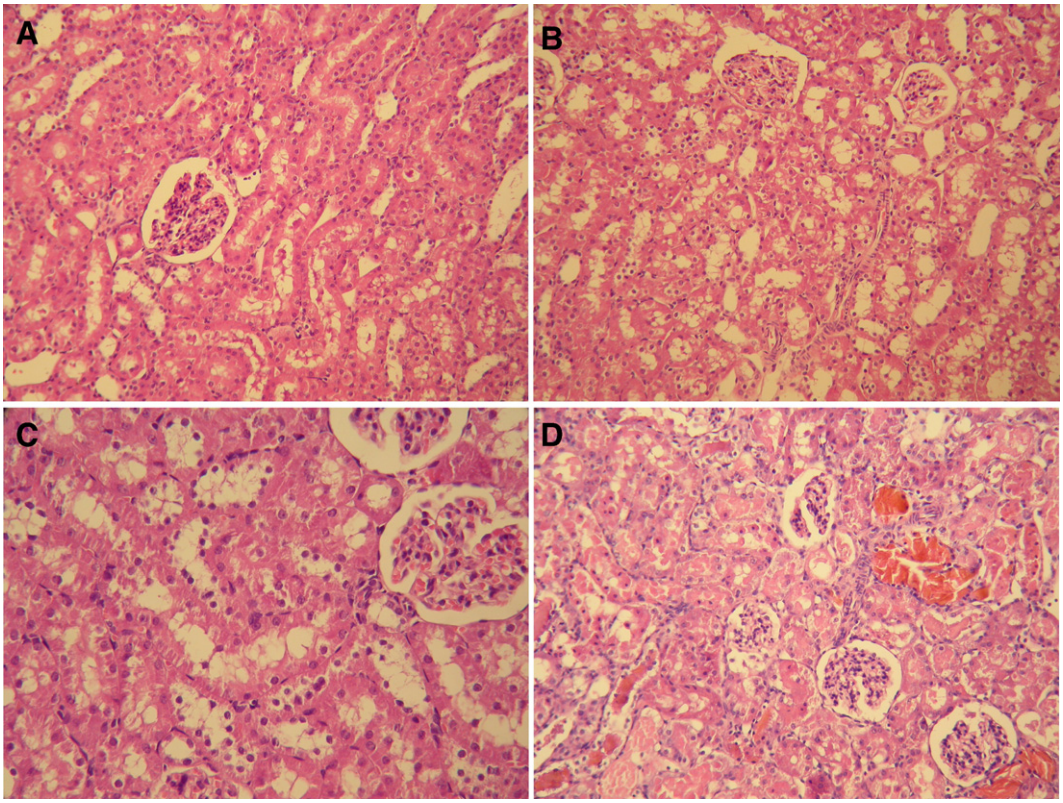

Fig. 5. Kidney histopathology of rats dosed with nano-copper particles (HE stain). (A) Control rats, with no abnormalities were noted. Magnification, 200×. (B) Low-dose (50 mg/kg/d) and (C) mid-dose (100 mg/kg/d) nano-copper-treated rats, the swelling proximal tubule was observed. Magnification, 200× and 400×, respectively. (D) High-dose nano-copper-treated (200 mg/kg/d) rat, the widespread proximal tubular necrosis, orange crystal matter were noted. Magnification, 400×. (For interpretation of the references to colour in this figure legend, the reader is referred to the web version of this article.)

hepatocytic necrosis in all rats of the 200 mg/kg/d group, and no overt sign of toxicity was found in either the mid- or low-dose nano-copper group (Fig. 4B). Significant damages were observed in the renal tissue acquired from the rats treated with nano-copper. For all rats dosed with 200 mg/kg/d nano-copper, the changes were characterized by widespread renal proximal tubule necrosis involving most of the nephrons; further, cellular fragments were found in the tubule lumen, where orange crystal matter deposition was commonly observed (Fig. 5D). Nano-copper (50 or 100 mg/kg/d) only caused the swelling of the proximal tubule epithelia in 2/6 and 6/6 rats, respectively (Figs. 5B, C).

^{1}H NMR spectroscopic and pattern recognition analysis of urine

Applying PC analysis to the data set of the day 1 urine spectra, the score plot (Fig. 6A) showed that the high-dose nano-copper group was clearly separated from the control group primarily in PC1. The corresponding loadings plot (Fig. 6B) showed that the decrease in the citrate (δ 2.54, 2.7) and 2-oxoglutarate (δ 2.42, 3.02) signals were responsible for this shift. NMR urinalysis indicated that the alterations in urinary metabolites induced by a high dose of nano-copper became more obvious on day 5. Elevated glucose, amino acid, citrate, succinate, lactate, acetate, and TMAO together with the decline in creatinine level were obvious in urine spectra obtained from the rats of the high-dose nano-copper group (Fig. 7). Mid- and low-dose groups also demonstrated a slight separation compared with the control, and a decrease in the citrate (δ 2.54, 2.7) and 2-oxoglutarate (δ 2.42, 3.02) signals were identified.

^{1}H NMR spectroscopic and pattern recognition analysis of serum

^{1}H NMR spectra of serum included spin-echo NMR spectra and diffusion-edited NMR spectra. They reflected the lower-molecular-weight and macromolecular-weight metabolites present in the serum. ^{1}H chemical shifts and assignments of endogenous metabolites in serum were conducted according to previous literature (Liao et al., 2007; Lindon et al., 1999). The PCA scores plot (Fig. 8A) derived from the ^{1}H NMR serum spectra of low-molecular-weight metabolites showed that only the high-dose nano-copper group was clearly separated from the control group. The metabolites discriminating this separation included lactate (δ 1.34), 3-hydroxybutyrate (δ 0.9, 1.7), acetate (δ 1.94), and creatine (δ 3.98), whose levels increased, and glucose (δ 3.46) and glutamine (δ 2.1, 2.42), whose levels were decreased (Fig. 8B).

The PCA scores plot from the ^{1}H NMR serum spectra of macromolecular-weight metabolites showed (Fig. 8C) that the high-dose nano-copper group was separated from the control group along PC1 and PC3. Additionally, the separation of the nano-copper mid- and low-dose groups from the control group along PC1 was also observed. A variety of biochemical changes were identified from the analysis of the corresponding loadings plot and NMR spectra. A marked increase in the intensity of triglycerides CH_3–(CH_2)n (δ 0.9), (CH_2)n (δ 1.26), CH_2CH_2*CO (δ 1.58), CH_2CO (δ 2.26), CH_2OCOR (δ 4.3), C=CCH_2C=C (δ 2.78), and CH=CH (δ 5.34) along with an increase in the signal of the phosphatide $CH_2OPO_2^-$ (δ 4.1) were responsible for the separation of the high-dose group. The elevation in the signals of (CH_2)n (δ 1.26), CH_2CO (δ 2.26), C=CCH_2C=C (δ 2.78), and CH=CH (δ 5.34) contributed to the separation of the mid- and low-dose groups (Fig. 8D).

^{1}H NMR spectroscopic and pattern recognition analysis of liver and kidney tissue

^{1}H NMR spectroscopic analysis of the aqueous extracts from the liver and kidney tissue obtained from the rats in the treated and

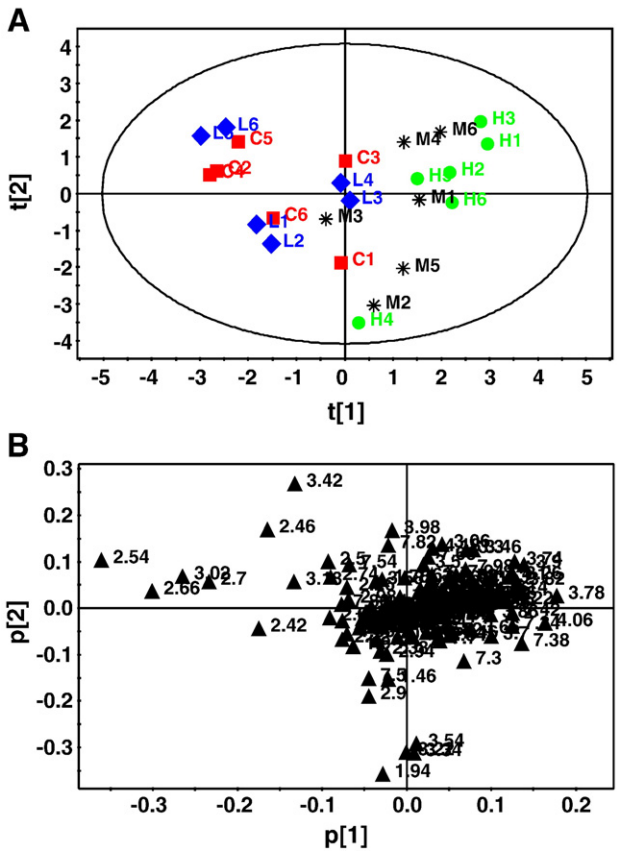

Fig. 6. (A) PCA scores plot based on ^{1}H NMR spectra of urine samples from rats on day 1. (B) PCA loadings plot corresponding to Fig. 6A. Key: C, control group; L, nano-copper: 50 mg/kg/d; M, nano-copper: 100 mg/kg/d; H, nano-copper: 200 mg/kg/d.

control groups by PCA indicated clear separation of the high-dose nano-copper group from the control group in their scores plots (Figs. 9A, B). Increased creatine (δ 3.06, 3.94) and decreased glutamine (δ 2.14, 2.46) and taurine (δ 3.26) was found in the liver aqueous extracts, and elevated lactate (δ 1.34) and reduced taurine (δ 3.26, 3.42) and glucose (δ 3.4–4.1) were identified in the kidney aqueous extracts (Figs. 10A, B).

^{1}H NMR spectra of the chloroform and methanol extracts of the liver and kidney tissues were dominated by a range of lipid moieties, including saturated and unsaturated triglycerides, and phosphatide. PC analysis indicated the apparent biochemical changes, including elevated signal intensity of the triglycerides CH_3–$(CH_2)n$ (δ 0.84), $(CH_2)_n$ (δ 1.24), and C=CCH_2C=C (δ 2.8) in the treated groups (Figs. 10C, D).

Discussion

In the current work, a number of toxicity manifestations, including anorexia, diarrhea, lethargy, and significant body-weight loss, observed in all rats dosed with 200 mg/kg/d nano-copper were similar to the effects of excessive copper compound treatment (Semple et al., 1960; Winge and Mehra, 1990; Hébert et al., 1993; Barceloux, 1999). However, the symptoms observed in the mid- and low-treated groups were insignificant. Here, the damages in the liver and kidneys found in rats dosed with nano-copper will be discussed in detail. In the case of rats in the high-dose nano-copper group, an elevation in the serum plasma enzyme aspartate aminotransferase and alanine aminotransferase as well as the plasma metabolite bilirubin suggested the presence of marked liver damage, which was further confirmed by the scattered dot hepatocytic necrosis. The kidney weight of rats in the high-dose group was significantly higher than that of the control rats. An increase in blood urea nitrogen and creatinine suggested a dysfunction in renal glomerular filtration. Widespread renal proximal tubule cell necrosis was also observed histopathologically. As for the mid- and low-dose groups, only a slight increase in serum cholesterol and triglycerides as well as the swelling of proximal tubule epithelia were observed. The above manifestations of the hepato- and nephrotoxicity induced by copper nanoparticles were consistent with the previous studies about oral ingestion of excess copper compounds (Haywood, 1980; Haywood and Comerford, 1980; Haywood et al., 1985a, b; NTP, 1993).

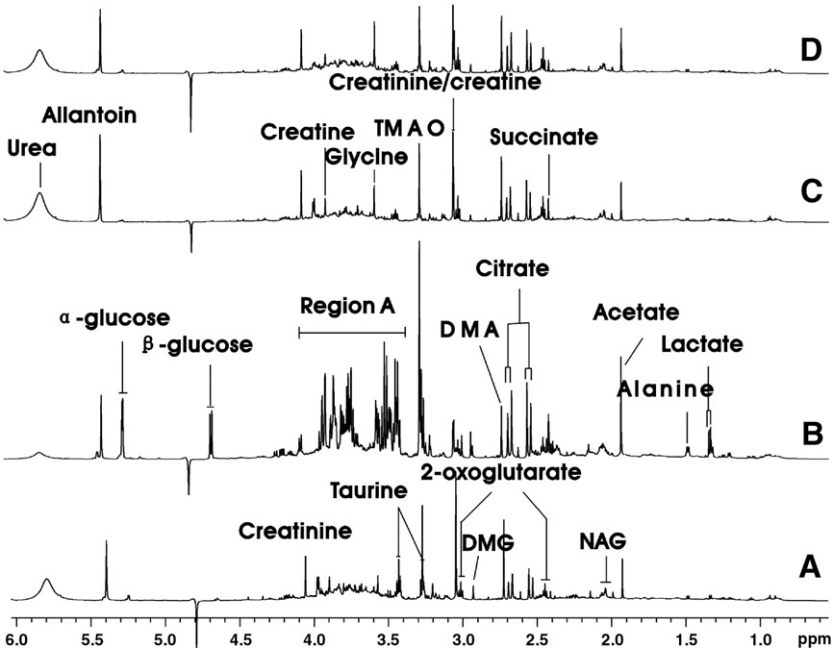

Fig. 7. ^{1}H NMR spectra of urine samples from rats treated with nano-copper for 5 d at doses of (B) 200 mg/kg, (C) 100 mg/kg/d, (D) 50 mg/kg/d, and (A) control. Key: DMA, dimethylamine; DMG, dimethylglycine; NAG, *N*-acetylglucosaminidase; Region A, signals from glycerol, glucose, and amino acid; TMAO, trimethylamine-*N*-oxide.

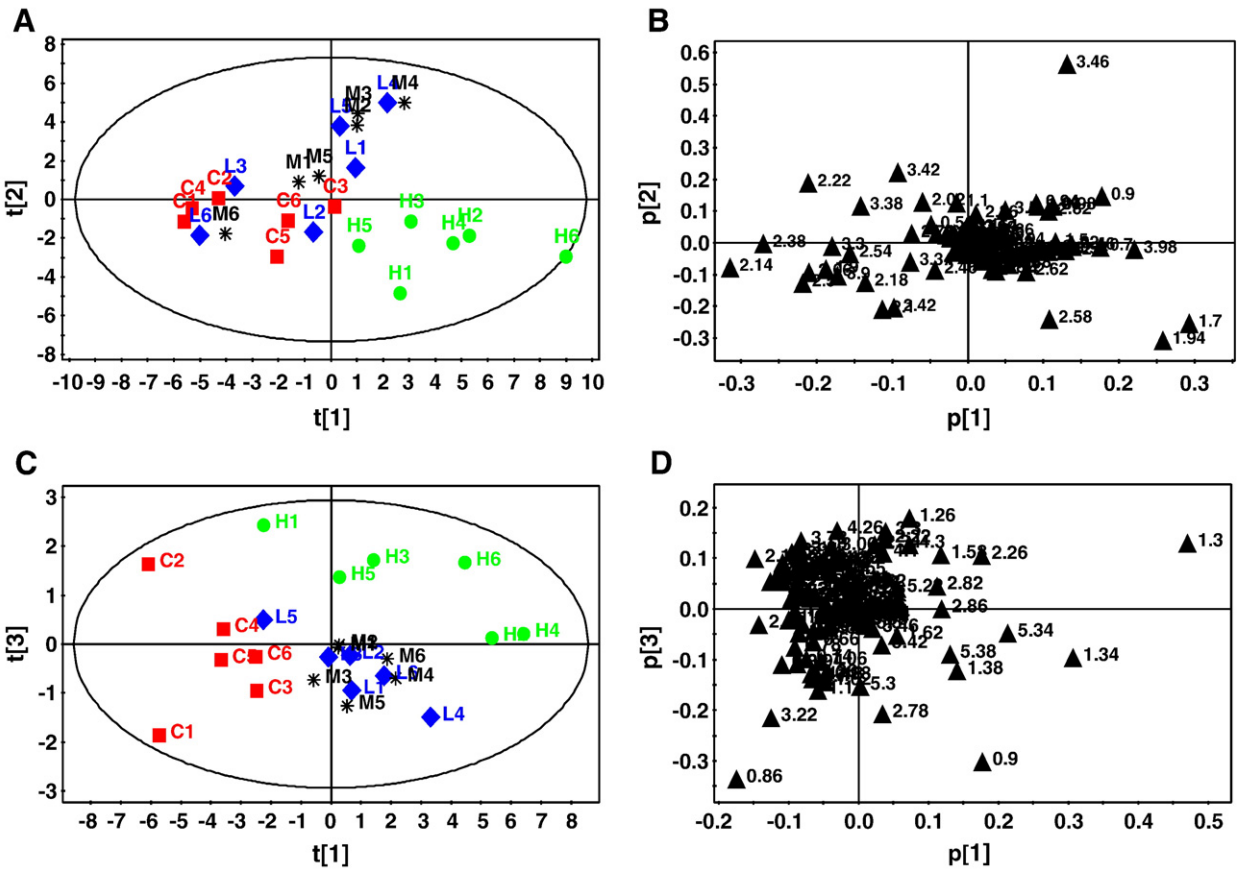

Fig. 8. (A and C) PCA scores plots based on spin-echo and diffusion-edited ^{1}H NMR spectra of serum samples from control and treated rats on day 6; (B and D) PCA loadings plots corresponding to Figs. 8A and C. Key: C, control group; L, nano-copper: 50 mg/kg/d; M, nano-copper: 100 mg/kg/d; H, nano-copper: 200 mg/kg/d.

The metabolic profile analysis for the samples of serum, urine, and extracts obtained from the liver and kidney tissue not only supported the above findings but also further revealed the information underlying hepato- and nephrotoxicity of nano-copper. Reduced citrate and 2-oxoglutarate was detected in the urine collected after the first 24 h from rats treated with 200 mg/kg nano-copper. Until day 5, similar changes in urine metabolites were observed in rats of the mid- and low-dose group rats. Citrate and 2-oxoglutarate are intermediates in the tricarboxylic acid cycle (TCA). This alteration reflected a common nonspecific effect of toxicity. We speculate that the uptake, distribution, and elimination relevant to nano-copper might increase the energy demand.

Under normal conditions, almost all glucose and low-molecular amino acids can be reabsorbed by renal proximal tubules. Both citrate and lactate are freely filtered by the glomerulus and reabsorbed by the renal proximal tubule. Citrate reabsorption occurs via an apical membrane Na^{+}/citrate cotransporter (Melnick et al., 1996), while lactate is reabsorbed along with glucose in the S1/S2 regions of the proximal tubule (Anthony et al., 1992). In this study, evident glucouria and aminoaciduria together with a marked increase in the level of urine lactate and citrate was observed in rats dosed with 200 mg/kg/d nano-copper for 5 d; this suggested the acute impairment in the renal proximal tubule and a reduction in the reabsorption ability from the tubule lumen in these rats. Additionally, creatine was found exceeding normal levels in both blood and tissue, which is a sign of renal insufficiency, and mainly reflects lower rates of glomerulus filtration (Feng et al., 2002). Markedly increased creatine in serum and aqueous extracts of liver tissue was consistent with hypocreatinuria. These findings further supported the occurrence of the dysfunction in renal glomerular filtration.

The disturbance of energy metabolism including anaerobic glycolysis, enhanced fatty acid β-oxidation and ketogenesis was related to the hepatotoxicity and nephrotoxicity in the rats treated with 200 mg/kg nano-copper for 5 d. Increased serum lactate were observed in the rats of high-dose nano-copper group, it is a consequence of anaerobic metabolism, and this metabolic pathway mainly provide ATP for the contracting skeletal muscle and brain activity and utilized during hepatic gluconeogenesis in periods of reduced energy availability. Ketones, such as plasma 3-hydroxybutyrate, are indicative of enhanced β-oxidation and can be utilized as an alternative energy source when glucose is limited. Acetate is an end product of fatty acid oxidation. In this study, increases in serum 3-hydrobutyrate and serum acetate levels denoted a shift in energy metabolism toward fatty acid β-oxidation and ketogenesis; this was consistent with the anorexia and hypoglycemia observed in the rats treated with a high dose of nano-copper. We deduced that two main aspects were contributed to the initiation and progress of energy disturbance. They involved excessive copper accumulation in the hepato- and nephrocytes via the direct action of copper and as a secondary result of marked reduction in food consumption in these animals. At present, the mechanism of cellular copper toxicity was considered to be primarily a result of the metal's ability to catalyze the formation of toxic oxygen species through a series of redox reactions (Samuni et al., 1981; Goldstein and Czapski, 1986; Stacey and Klaassen, 1981). Mitochondria are the preferential target of oxidative injury. Based on this information, we deduced that excessive copper accumulation in hepatocytes or nephrocytes would inevitably result in mitochondrial failure and cell death. Thus, interruption of the oxidative phosphorylation pathway would directly affect the ATP-generation. In addition, the latest study indicated that acute caloric restriction can induce the metabolic shift in transcription toward fatty acid catabolism, β-oxidation, and gluconeogenesis and away from lipid biosynthetic processes in both the liver

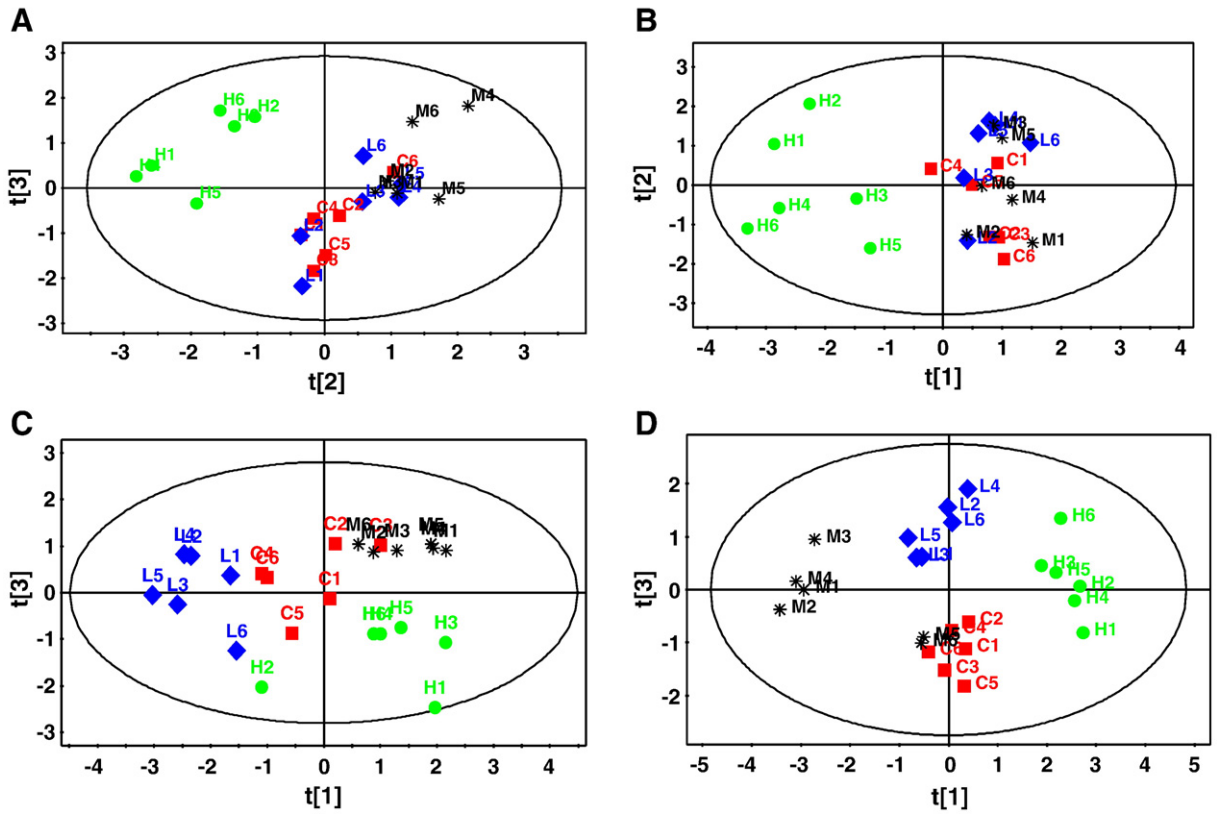

Fig. 9. PCA scores plots based on the ^{1}H NMR spectra of liver tissue aqueous extracts and lipid soluble liver extracts on day 6 (A and B); PCA scores plots based on ^{1}H NMR spectra of kidney aqueous extracts and lipid soluble kidney extracts on day 6 (C and D). Key: C, control group; L, nano-copper: 50 mg/kg/d; M, nano-copper: 100 mg/kg/d; H, nano-copper: 200 mg/kg/d.

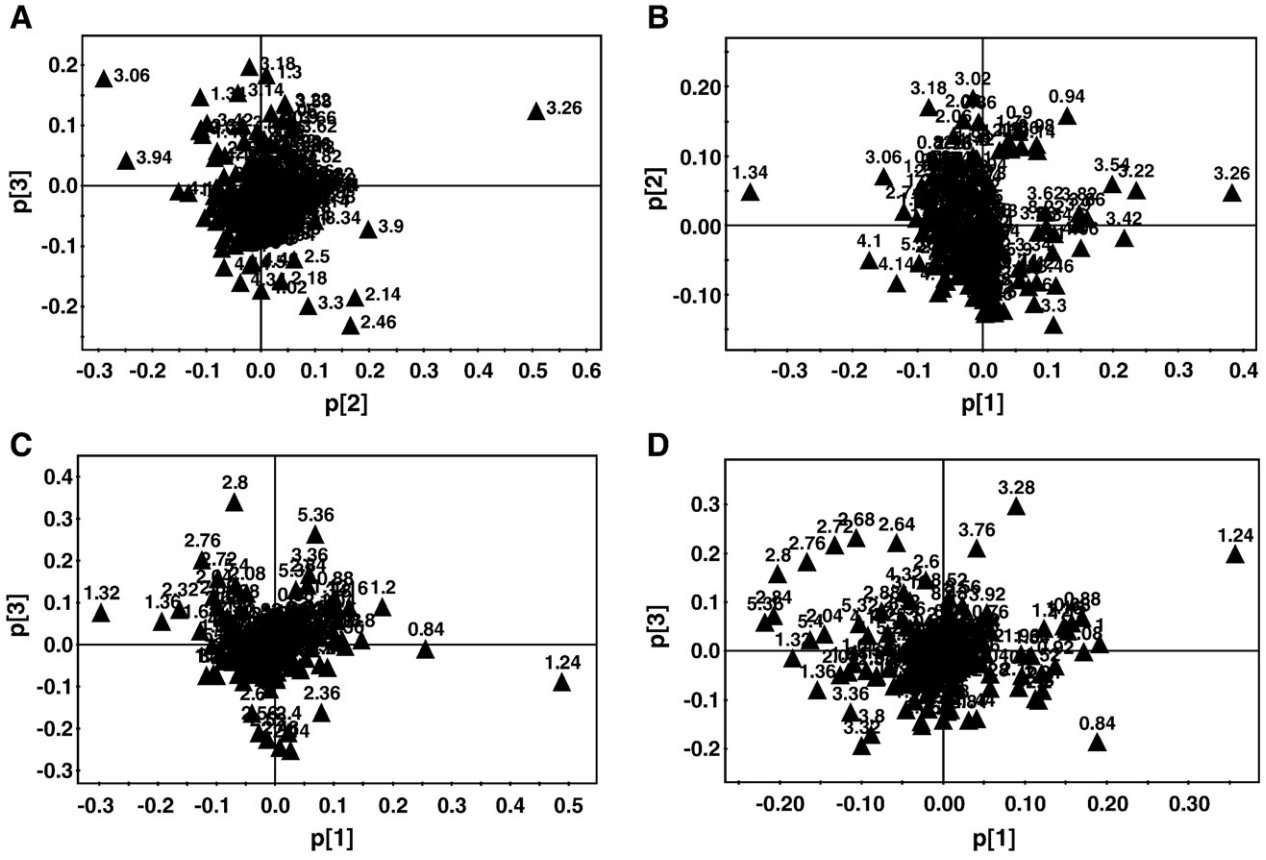

Fig. 10. PCA loadings plots based on ^{1}H NMR spectra of liver tissue aqueous extracts and lipid soluble liver extracts on day 6 (A and B). PCA scores plots based on ^{1}H NMR spectra of kidney tissue aqueous extracts and lipid soluble kidney extracts on day 6 (C and D).

and muscle. In agreement, the alteration of plasma metabolites included increases in lactate, 3-hydroxybutyrate, cholesterol, associated low-density lipoprotein levels, and several glucogenic amino acids (methionine, glutamine, alanine, valine). Plasma concentrations of glucose and choline were decreased during acute caloric restriction, as were the resonances of lipids including very low-density lipoproteins (Selman et al., 2006). By comparing the serum biomarkers taken from acute calorie restriction and nano-copper exposure, we can find that the general tendency of the energy metabolism alteration between them was in agreement, but acute caloric restriction could not give an elegant explanation about the changes of the serum lipid species in the rats treated with nano-copper at the lower doses.

The levels of serum (CH_2)n, CH_2CO, $C{=}CCH_2C{=}C$, and CH=CH was observed in rats treated with nano-copper; this indicated defective lipid metabolism in these rats. There was a correlated increase in the intensity of CH_3–(CH_2)n, $(CH_2)_n$, and $C{=}CCH_2C{=}C$ in the chloroform/methanol extracts of the liver and kidney tissue of rats in the nano-copper treated groups and a rise in the level of serum phosphatide $CH_2OPO_2^-$ in rats of the high-dose group. These results were further supported by the defective lipid metabolism induced by nano-copper. Similar lesions have been reported in rats due to excessive copper ingestion, but there were certain inconsistencies in the results. High dietary Cu was shown to increase the amount of unsaturation in porcine back fat (Ho and Elliot, 1974). Increased cholesterol and decreased triglyceride were observed in both the serum and liver of rats after administration of cupric ions (Tanaka et al., 1987). Cu supplements (10, 20, and 50 ppm) in the diet diminished the cholesterol and triglyceride serum levels and increased the level of phospholipids (Alarcón et al., 2000). A recent study reported that copper can selectively downregulate lipid metabolism, particularly cholesterol biosynthesis (Huster et al., 2007). We speculated that the exposure to different doses at different times may explain the discrepancies among of these copper-related disorders in lipid metabolism to some extent. In the current work, we deduced that lipid metabolism disorders might also be partly attributed to oxidation stress, based on the previous study (Galhardi et al., 2004). Additionally, increased serum phosphatide in rats of the high-dose group might be related to the breakdown of cell membrane-like constituents as hepatocytic and renal proximal tubule cell necrosis. These findings also indicate that NMR analysis of serum and tissue extracts enables detection of a toxicologically relative change (lipidosis) that cannot be detected by histopathology.

In this study the damage in the liver and kidney suggested the presence of a copper overload; our subsequent work has also demonstrated that the copper content significantly increased in the liver or kidney tissue in the case of rats that were administered 200 mg/kg/d nano-copper (data not shown). In vitro dissolution analysis of nano-copper in artificial gastric fluid supported that a slight amount of nano-copper was transformed into copper ions in the rat stomach when they were ingested. Furthermore, the large surface area of the nanoparticles means its strong adsorbability. We speculated that rats multi-treated with 200 mg/kg/d nano-copper orally might suffer from excessive accumulation of copper nanoparticles in the gastrointestinal tract and a delay in gastric emptying. It would encourage further production of ionic copper. Previous literature indicated that Cu(I) strikingly rapidly (<1 s) in an aqueous solution to form Cu(II) and Cu(0) (Cotton and Wilkinson, 1980). We reasonably thought that ionic copper transformed from nano-copper was predominantly cupric. Cupric was readily absorbed from the stomach and small intestine into blood (Turnlund et al., 1997). Therefore, the copper overload in the target organs could be partly attributed to cupric. To date, it is unclear whether nano-copper can enter into the blood circulation through the intact gastrointestinal lining. In this study, the situation which the acute gastroenteritis accompanied by severe diarrhea occurring in the rats treated with a high dose of nano-copper might facilitate the absorption of nano-copper into blood and its translocation thereafter into the liver and other organs. If soluble ionic copper could be slowly released over time from tissue accumulations acting as toxic reservoirs, this nano-copper would exhibit some different biological characteristics compared to its soluble counterparts. This hypothesis however requires further investigation.

In summary, our work demonstrated both the toxicity and the damages in liver and kidney induced by nano-copper and confirmed that these manifestations were similar to those of its soluble counterpart cupric *in vivo*. Rats were repeatedly treated with an oral dose of nano-copper for a short term, 50 mg/kg/d was close to the lowest observed adverse effect level. The changes in metabolic components suggested mitochondrial failure, and enhanced ketogenesis, fatty acid β-oxidation, and glycolysis were said to contribute to hepatotoxicity and nephrotoxicity induced by a dose of 200 mg/kg/d nano-copper. The increase in triglycerides in the serum, liver and kidney tissue could serve as a potential sensitive biomarker reflecting the lipidosis induced by nano-copper. The data generated from the present study completely supports the fact that integrated metabolomic approach is promising for the development of rapid *in vivo* screening and for understanding the mechanism underlying the hepatotoxicity and nephrotoxicity of xenobiotics. The advantages of metabolomic approach, such as sensitive, timesaving and high-throughput, also favor it as a rapid *in vivo* screening method for nanotoxicity.

Acknowledgments

We wish to thank Yansheng Dong and Jiadi Shen for expert assistance in clinical chemistry examination and Qi Zhang for her aids with pattern recognition and PCA analysis. The authors acknowledge the funding support from National High-Tech Projects (2006CB705602).

References

Alarcón, C.O.M., Carnevalí, D.T.E., Reinosa, F.J., Contreras, Y., Ramírez, D.F.M., Yánez, D.C., 2000. Changes in serum lipids in rats treated with oral copper. Arch. Latinoam. Nutr. 50, 249–256.

Anthony, M.L., Gartland, K.P., Beddell, C.R., Lindon, J.C., Nicholson, J.K., 1992. Cephaloridine-induced nephrotoxicity in the Fischer 344 rat: proton NMR spectroscopic studies of urine and plasma in relation to conventional clinical chemical and histopathological assessments of nephronal damage. Arch. Toxicol. 66, 525–537.

Atherton, H.J., Bailey, N.J., Zhang, W., Taylor, J., Major, H., Shockcor, J., Clarke, K., Griffin, J.L., 2006. A combined ^{1}H-NMR spectroscopy–and mass spectrometry–based metabolomic study of the PPAR-α null mutant mouse defines profound systemic changes in metabolism linked to the metabolic syndrome. Physiol. Genomics 2, 178–186.

Bakunin, V.N., Suslov, A.Y., Kuzmina, G.N., Parenago, O.P., Topchiev, A.V., 2004. Synthesis and application of inorganic nanoparticles as lubricant. Components. J. Nanopart. Res. 2, 273–284.

Barceloux, D.G., 1999. Copper. J. Toxicol. Clin. Toxicol. 37, 217–237.

Bremner, I., 1998. Manifestations of copper excess. Am. J. Clin. Nutr. 67, 1069–1073.

Chen, Z., Meng, H., Xing, G.M., Chen, C.Y., Zhao, Y.L., Jia, G., Wang, T.C., Yuan, H., Ye, C., Zhao, F., Chai, Z.F., Zhu, C.F., Fang, X.H., Ma, B.C., Wan, L.J., 2006. Acute toxicological effects of copper nanoparticles in vivo. Toxicol. Lett. 163, 109–120.

Cioffi, N., Ditaranto, N., Torsi, L., Picca, R.A., Sabbatini, L., Valentini, A., Novello, L., Tantillo, G., Bleve-Zacheo, T., Zambonin, P.G., 2005. Analytical characterization of bioactive fluoropolymer ultra-thin coatings modified by copper nanoparticles. Anal. Bioanal. Chem 381, 607–616.

Coen, M., Ruepp, S.U., Lindon, J.C., Nicholson, J.K., Pognan, F., Lenz, E.M., Wilson, I.D., 2004. Integrated application of transcriptomics and metabonomics yields new insight into the toxicity due to paracetamol in the mouse. J. Pharm. Biomed. Anal. 35, 93–105.

Colvin, V., 2003. The potential environmental impact of engineered nanomaterials. Nat. Biotechnol. 21, 1166–1170.

Cotton, F.A., Wilkinson, G., 1980. Copper. Advanced Inorganic Chemistry. John Wiley and Sons, New York, NY, pp. 798–821.

Dunn, W.B., Bailey, N.J., Johnson, H.E., 2005. Measuring the metabolome: current analytical technologies. Analyst 130, 606–625.

Feng, J., Li, X., Pei, F., Chen, X., Li, S., Nie, Y., 2002. ^{1}H NMR analysis for metabolites in serum and urine from rats administrated chronically with $La(NO_3)_3$. Anal. Biochem. 301, 1–7.

Galhardi, C.M., Diniz, Y.S., Faine, L.A., Rodrigues, H.G., Burneiko, R.C., Ribas, B.O., Novelli, E.L., 2004. Toxicity of copper intake: lipid profile, oxidative stress and susceptibility to renal dysfunction. Food Chem. Toxicol. 42, 2053–2060.

Gartland, K.P., Beddell, C.R., Lindon, J.C., Nicholson, J.K., 1991. Application of pattern recognition methods to the analysis and classification of toxicological data derived from proton nuclear magnetic resonance spectroscopy of urine. Mol. Pharmacol. 139, 629–642.

Goldstein, S., Czapski, G., 1986. The role and mechanism of metal ions and their complexes in enhancing damage in biological systems or in protecting these systems from the toxicity of O^{2-}. J. Free Radic. Bio. Med. 2, 3–11.

Haywood, S., 1980. The effect of excess dietary copper on the liver and kidney of the male rat. J. Comp. Pathol. 90, 217–232.

Haywood, S., Comerford, B., 1980. The effect of excess dietary copper on plasma enzyme activity and on the copper content of the blood of the male rat. J. Comp. Pathol. 90, 233–238.

Haywood, S., Loughran, M., Batt, R.M., 1985a. Copper toxicosis and tolerance in the rat. III. Intracellular localization of copper in the liver and kidney. Exp. Mol. Pathol. 43, 209–219.

Haywood, S., Trafford, J., Loughran, M., 1985b. Copper toxicosis and tolerance in the rat. IV. Renal tubular excretion of copper. Br. J. Exp. Pathol. 66, 699–707.

Hébert, C.D., Elwell, M.R., Travlos, G.S., Fitz, C.J., Bucher, J.R., 1993. Subchronic toxicity of cupric sulfate administered in drinking water and feed to rats and mice. Fundam. Appl. Toxicol. 21, 461–475.

Ho, S.K., Elliot, J.I., 1974. Fatty acid composition of porcine depot fat as related to the effect of supplemental dietary copper on the specific activities of fatty acyl desaturase system. Can. J. Anim. Sci. 54, 23–28.

Holmes, E., Foxall, P.J.D., Nicholson, J.K., Neild, G.H., Brown, S.M., Beddell, C.R., Sweatman, B.C., Rahr, E., Lindon, J.C., Spraul, M., Neidig, P., 1994. Automatic data reduction and pattern recognition methods for analysis of ^{1}H nuclear magnetic resonance spectra of human urine from normal and pathological states. Anal. Biochem. 220, 284–296.

Holmes, E., Nicholls, A.W., Lindon, J.C., Ramos, S., Spraul, M., Neidig, P., Connor, S.C., Connelly, J., Damment, S.J., Haselden, J., Nicholson, J.K., 1998. Development of a model for classification of toxin-induced lesions using ^{1}H NMR spectroscopy of urine combined with pattern recognition. NMR Biomed. 11, 235–244.

Holmes, E., Nicholls, A.W., Lindon, J.C., Connor, S.C., Connelly, J.C., Haselden, J.N., Damment, S.J., Spraul, M., Neidig, P., Nicholson, J.K., 2000. Chemometric models for toxicity classification based on NMR spectra of biofluids. Chem. Res. Toxicol. 13, 471–478.

Huster, D., Purnat, T.D., Burkhead, J.L., Ralle, M., Fiehn, O., Stuckert, F., Olson, N.E., Teupser, D., Lutsenko, S., 2007. High copper selectively alters lipid metabolism and cell cycle machinery in the mouse model of Wilson disease. J. Biol. Chem. 282, 8343–8355.

Liao, P., Wei, L., Zhang, X., Li, X., Wu, H., Wu, Y., Ni, J., Pei, F., 2007. Metabolic profiling of serum from gadolinium chloride-treated rats by ^{1}H NMR spectroscopy. Anal. Biochem. 364, 112–121.

Lindon, J.C., Nicholson, J.K., Everett, J.R., 1999. NMR spectroscopy of biofluids. Annu. Rep. NMR Spectrosc. 38, 1–88.

Lindon, J.C., et al., 2005. Standardization of Reporting Methods for Metabolic Analyses: A Draft Policy Document from the Standard Metabolic Reporting Structures (SMRS) Group, v2.3. Appendix 5, Typical NMR data acquisition and pre-processing parameters. Imperial College, London, UK,.

Liu, G., Li, X., Qin, B., Xing, D., Guo, Y., Fan, R., 2004. Investigation of the mending effect and mechanism of copper nanoparticles on a tribologically stressed surface. Tribology Lett. 17, 961–966.

Maxwell, R.J., Martinez-Perez, I., Cerdan, S., Cabanas, M.E., Arus, C., Moreno, A., Capdevila, A., Ferrer, E., Bartomeus, F., Aparicio, A., Conesa, G., Roda, J.M., Carceller, F., Pascual, J.M., Howells, S.L., Mazucco, R., Griffiths, J.R., 1998. Pattern recognition analysis of ^{1}H NMR spectra from perchloric acid extracts of human brain tumor biopsies. Magn. Reson. Med. 39, 869–877.

Melnick, J.Z., Srere, P.A., Elshourbagy, N.A., Moe, O.W., Preisig, P.A., Alpern, R.J., 1996. Adenosine triphosphate citrate lyase mediates hypocitraturia in rats. J. Clin. Invest. 98, 2381–2387.

Meng, H., Chen, Z., Xing, G.M., Yuan, H., Chen, C.Y., Zhao, F., Zhang, C.C., Zhao, Y.L., 2007. Ultrahigh reactivity provokes nanotoxicity: explanation of oral toxicity of nanocopper particles. Toxicol. Lett. 175, 102–110.

Nicholson, J.K., Connelly, J., Lindon, J.C., Holmes, E., 2002. Metabonomics: a platform for studying drug toxicity and gene function. Nat. Rev. Drug. Disc. 1, 153–161.

NTP, 1993. NTP Technical Report on toxicity studies of cupric sulfate administered in drinking water and feed to F344/N rats and B6C3F1 mice. National Toxicology Program. United States Department of Health and Human Services. NIH Publication 93-3352.

Robertson, D.G., Reily, M.D., Sigler, R.E., Wells, D.F., Paterson, D.A., Braden, T.K., 2000. Metabonomics: evaluation of nuclear magnetic resonance (NMR) and pattern recognition technology for rapid in vivo screening of liver and kidney toxicants. Toxicol. Sci. 57, 326–337.

Samuni, A., Chevion, M., Czapski, G., 1981. Unusual copper-induced sensitization of the biological damage due to superoxide radicals. J. Biol. Chem. 256, 12632–12635.

Selman, C., Kerrison, N.D., Cooray, A., Piper, M.D.W., Lingard, S.J., Barton, R.H., Schuster, E.F., Blanc, E., Gems, D., Nicholson, J.K., Thornton, J.M., Partridge, L., Withers, D.J., 2006. Coordinated multitissue transcriptional and plasma metabonomic profiles following acute caloric restriction in mice. Physiol. Genomics 27, 187–200.

Semple, A.B., Parry, W.H., Philips, D.E., 1960. Acute copper poisoning: an outbreak traced to contaminated water from a corroded geyser. Lancet 2, 700–701.

Serkova, N.J., Niemann, C.U., 2006. Pattern recognition and biomarker validation using quantitative ^{1}H-NMR-based metabolomics. Expert Rev. Mol. Diagn. 6, 717–731.

Stacey, N.H., Klaassen, C.D., 1981. Copper toxicity in isolated rat hepatocytes. Toxicol. Appl. Pharmacol. 58, 211–220.

Tanaka, M., Iio, T., Tabata, T., 1987. Effect of cupric ions on serum and liver cholesterol metabolism. Lipids 22, 1016–1019.

Turnlund, J.R., Scott, K.C., Peiffer, G.L., Jang, A.M., Keyes, W.R., Keen, C.L., Sakanashi, T.M., 1997. Copper status of young men consuming a low-copper diet. Am. J. Clin. Nutr. 65, 72–78.

Want, E.J., Nordström, A., Morita, H., Siuzdak, G., 2007. From exogenous to endogenous: the inevitable imprint of mass spectrometry in metabolomics. J. Proteome. Res. 6, 459–468.

Waters, N.J., Waterfield, C.J., Farrant, R.D., Holmes, E., Nicholson, J.K., 2005. Metabonomic deconvolution of embedded toxicity: application to thioacetamide hepato- and nephrotoxicity. Chem. Res. Toxicol. 18, 639–654.

Waters, N.J., Waterfield, C.J., Farrant, R.D., Holmes, E., Nicholson, J.K., 2006. Integrated metabonomic analysis of bromobenzene-induced hepatotoxicity: novel induction of 5-oxoprolinosis. J. Proteome. Res. 5, 1448–1459.

Waterfield, C.J., Turton, J.A., Scales, M.D., Timbrell, J.A., 1993. Investigations into the effects of various hepatotoxic compounds on urinary and liver taurine levels in rats. Arch. Toxicol. 67 (4), 244–254.

Winge, D.R., Mehra, R.K., 1990. Host defenses against copper toxicity. Int. Rev. Exp. Pathol. 31, 47–83.

Yap, I.K., Clayton, T.A., Tang, H., Everett, J.R., Hanton, G., Provost, J.P., Le, N.J.L., Charuel, C., Lindon, J.C., Nicholson, J.K., 2006. An integrated metabonomic approach to describe temporal metabolic disregulation induced in the rat by the model hepatotoxin allyl formate. J. Proteome. Res. 5, 2675–2684.